Non perturbative chiral approach to s-wave $\bar{K}N$ interactions

E. Oset

Departamento de Física Teórica and IFIC, Centro Mixto Universidad de Valencia-CSIC,

46100 Burjassot (Valencia), Spain

A. Ramos

Departament d'Estructura i Constituents de la Matèria, Universitat de Barcelona,

Diagonal 647, 08028 Barcelona, Spain

(February 9, 2008)

Abstract

The s-wave meson-nucleon interaction in the $S = -1$ sector is studied by means of coupled-channel Lippmann Schwinger equations, using the lowest order chiral Lagrangian and a cut off to regularize the loop integrals. The method reproduces succesfully the $\Lambda(1405)$ resonance and the $K^-p \rightarrow K^-p, \bar{K}^0 n, \pi^0 \Lambda, \pi^0 \Sigma, \pi^+ \Sigma^-, \pi^- \Sigma^+$ cross sections at low energies. The inclusion of the $\eta \Lambda, \eta \Sigma^0$ channels in the coupled system is found very important and allows a solution in terms of only the lowest order Lagrangian.

Typeset using REVTEX

I. INTRODUCTION

The effective chiral Lagrangian formalism which has proved successful in explaining the properties of meson-meson interaction at low energies [1–3] has also proved to be an idoneous tool to study low energy properties of the meson-baryon interaction [4,5]. The s-wave πN and $K^+ N$ interaction is relatively weak and the leading term in the chiral expansion $O(q)$ is the dominant one [6,7]. By contrary, in the $S = -1$ sector, the $\bar{K}N$ system couples strongly to many other channels and generates a resonance below threshold in s-wave, the $\Lambda(1405)$. In such case the standard chiral perturbative scheme, an expansion in powers of the typical momenta involved in the process, fails to be an appropiate approach, since the singularities of the T matrix associated to the resonance cannot be generated perturbatively.

A non perturbative scheme to the $S = -1$ meson-baryon sector, yet using the input of the Chiral Lagrangians, was employed in [8]. A set of coupled-channel Lippmann Schwinger (LS) equations was solved using the lowest and next to lowest order chiral Lagrangians. The $\Lambda(1405)$ resonance was generated and the cross sections of the $K^- p \rightarrow K^- p, \bar{K}^0 n, \pi^0 \Lambda, \pi^+ \Sigma^-, \pi^0 \Sigma^0, \pi^- \Sigma^+$ reactions at low energies, plus the threshold branching ratios, were well reproduced. In summary, five parameters were needed to fit the experimental information, corresponding to, so far, unknown parameters of the second order chiral Lagrangian plus some range parameters used to construct a potential from the chiral Lagrangians. The method was also used to study coupled channels in the πN sector plus eta meson and kaon photoproduction in [9]. The role of the resonance is so important in $\bar{K}N$ scattering at low energies that any finite-order chiral expansion will fail to reproduce the data, unless the $\Lambda(1405)$ is introduced as an elementary matter field [10]. Another approach based on the coupled-channel LS equations [11] started from transition potentials whose relative strength between various channels was guided by SU(3) symmetry but was allowed to be broken by up to $\pm 50\%$ in order to fit the data.

The success of Ref. [8] has stimulated work in the meson-meson sector. In [12] similar ideas were followed and, by means of coupled-channel LS equations using the lowest order

chiral Lagrangian, plus a suitable cut off in the loops in order to simulate the effect of the second order Lagrangian, an excellent reproduction of the $\sigma, f_0(980), a_0(980)$ resonances in the scalar sector, plus phase shifts and inelasticities in the different physical channels was obtained. The work required just one free parameter, the cut off, q_{max}, in the momentum of the loop. However, the extension of these ideas to the $L = 1$ sector proved that the cut off alone was insufficient to account for the information contained in the second order chiral Lagrangians and the generation of the ρ and K^* resonances required further input.

In [13] the method of [12] was generalized using ideas of the inverse amplitude method [14,15] leading to a unitary coupled-channel non perturbative scheme that includes the works of [12] and [14,15] as particular cases. It uses the input of the first and second order Lagrangians and a cut off regularization and reproduces all the meson-meson experimental information up to $\sqrt{s} = 1.2\,\mathrm{GeV}$, including the resonances $\sigma, f_0(980), a_0(980), \rho$ and K^*. The work requires the use of 7 parameters, coefficients of the second order chiral Lagrangians in the meson-meson interaction [1].

In the present work we want to extend the ideas of [12] to the $\bar{K}N$ sector and investigate the possibility to describe all the low energy experimental cross sections plus the $\Lambda(1405)$ resonance in terms of the lowest order chiral Lagrangian (with no free parameters) and one cut off. As we shall see, we succeed in the enterprise, thus stressing the role of chiral symmetry in the meson-baryon interaction and at the same time the usefulness of the unitary coupled-channel method of [12] to deal with this kind of reactions.

The work presented here shares many points with [8] but has one different main result. The authors of [8] were able to reproduce fairly well the experimental cross sections with just the lowest order Lagrangian, but found substantial differences with the threshold branching ratios. We can reproduce all the results with the lowest order Lagrangian and one cut off. The main reason for the differences is the inclusion of two extra channels in our approach. In [8] the $K^-p, \bar{K}^0n, \pi^0\Lambda, \pi^+\Sigma^-, \pi^0\Sigma^0$ and $\pi^-\Sigma^+$ channels were considered. The $\eta\Lambda$ and $\eta\Sigma^0$ channels open up at higher K^- energies than studied in [8] and thus they were omitted in that work. We have included these channels in our approach using the analytical extrapolation of

these amplitudes below threshold and find substantial effects in the cross sections, changing the key threshold ratios in more than a factor two.

II. MESON-NUCLEON AMPLITUDES TO LOWEST ORDER

Following [3–5] we write the lowest order chiral Lagrangian, coupling the octet of pseudoscalar mesons to the octet of $1/2^+$ baryons, as

$$L_1^{(B)} = < \bar{B} i\gamma^\mu \nabla_\mu B > -M_B < \bar{B}B > +$$

$$\frac{1}{2}D < \bar{B}\gamma^\mu\gamma_5\{u_\mu, B\}> +\frac{1}{2}F < \bar{B}\gamma^\mu\gamma_5[u_\mu, B] > \tag{1}$$

where the symbol $<>$ denotes trace of SU(3) matrices and

$$\nabla_\mu B = \partial_\mu B + [\Gamma_\mu, B]$$
$$\Gamma_\mu = \tfrac{1}{2}(u^+\partial_\mu u + u\partial_\mu u^+)$$
$$U = u^2 = \exp(i\sqrt{2}\Phi/f) \tag{2}$$
$$u_\mu = iu^+\partial_\mu U u^+$$

The SU(3) matrices for the mesons and the baryons are the following

$$\Phi = \begin{pmatrix} \frac{1}{\sqrt{2}}\pi^0 + \frac{1}{\sqrt{6}}\eta & \pi^+ & K^+ \\ \pi^- & -\frac{1}{\sqrt{2}}\pi^0 + \frac{1}{\sqrt{6}}\eta & K^0 \\ K^- & \bar{K}^0 & -\frac{2}{\sqrt{6}}\eta \end{pmatrix} \tag{3}$$

$$B = \begin{pmatrix} \frac{1}{\sqrt{2}}\Sigma^0 + \frac{1}{\sqrt{6}}\Lambda & \Sigma^+ & p \\ \Sigma^- & -\frac{1}{\sqrt{2}}\Sigma^0 + \frac{1}{\sqrt{6}}\Lambda & n \\ \Xi^- & \Xi^0 & -\frac{2}{\sqrt{6}}\Lambda \end{pmatrix} \tag{4}$$

At lowest order in momentum, that we will keep in our study, the interaction Lagrangian comes from the Γ_μ term in the covariant derivative and we find

$$L_1^{(B)} = < \bar{B} i\gamma^\mu \frac{1}{4f^2}[(\Phi\partial_\mu\Phi - \partial_\mu\Phi\Phi)B - B(\Phi\partial_\mu\Phi - \partial_\mu\Phi\Phi)] > \tag{5}$$

4

which leads to a common structure of the type $\bar{u}\gamma^u(k_\mu+k'_\mu)u$ for the different channels, where $u, \bar{u}$ are the Dirac spinors and k, k' the momenta of the incoming and outgoing mesons.

We take the K^-p state and all those that couple to it within the chiral scheme. These states are $\bar{K}^0n, \pi^0\Lambda, \pi^0\Sigma^0, \pi^+\Sigma^-, \pi^-\Sigma^+, \eta\Lambda, \eta\Sigma^0$. Hence we have a problem with eight coupled channels. We should notice that, in addition to the six channels considered in [8] we have the two η channels, $\eta\Lambda$ and $\eta\Sigma^0$. Although these channels are above threshold for K^-p scattering at low energies, they couple strongly to the K^-p system and there are important interferences between the real parts of the amplitudes, which make their inclusion in the coupled-channel approach very important as we shall see.

The lowest order amplitudes for these channels are easily evaluated from eq. (5) and are given by

$$V_{ij} = -C_{ij}\frac{1}{4f^2}\bar{u}(p')\gamma^\mu u(p)(k_\mu + k'_\mu) \tag{6}$$

were $p, p'(k, k')$ are the initial, final momenta of the baryons (mesons). Also, for low energies one can safely neglect the spatial components in eq. (6) and only the γ^0 component becomes relevant, hence simplifying eq. (6) which becomes

$$V_{ij} = -C_{ij}\frac{1}{4f^2}(k^0 + k'^0) \tag{7}$$

The matrix C_{ij}, which is symmetric, is given in Table I.

III. ISOSPIN FORMALISM

We shall construct the amplitudes using the isospin formalism for which we must use average masses for the K $(K^-, \bar{K}^0)$, N (p, n), π (π^+, π^0, π^-) and Σ $(\Sigma^+, \Sigma^0, \Sigma^-)$ states. The isospin amplitudes are

$$| \bar{K}N, T = 0\rangle = \frac{1}{\sqrt{2}}(\bar{K}^0n + K^-p)$$
$$| \bar{K}N, T = 1\rangle = \frac{1}{\sqrt{2}}(\bar{K}^0n - K^-p) \tag{8}$$

5

$$| \pi\Sigma, T = 0 \rangle = -\frac{1}{\sqrt{3}}(\pi^+\Sigma^- + \pi^0\Sigma^0 + \pi^-\Sigma^+)$$

$$| \pi\Sigma, T = 1 \rangle = \frac{1}{\sqrt{2}}(\pi^-\Sigma^+ - \pi^+\Sigma^-) \, ,$$

where we use the phase convention $| \pi^+ \rangle = - | 1, 1 \rangle$, $| \Sigma^+ \rangle = - | 1, 1 \rangle$, $| K^- \rangle = - | 1/2, -1/2 \rangle$ for the isospin states, consistent with the structure of the Φ and B matrices.

In $T = 0$ we have three channels, $\bar{K}N, \pi\Sigma$ and $\eta\Lambda$ while in $T = 1$ we have four channels, $\bar{K}N, \pi\Sigma, \pi\Lambda, \eta\Sigma$. Using eqs. (8) and Table I we can construct the transition matrix elements in isospin formalism which read

$$V_{ij}(T = 0) = -D_{ij}\,\frac{1}{4f^2}\,(k^0 + k'^0)$$

$$V_{ij}(T = 1) = -F_{ij}\,\frac{1}{4f^2}\,(k^0 + k'^0) \tag{9}$$

and the symmetrical D_{ij}, F_{ij} coefficients are given in Tables II and III.

An alternative treatment can be done using directly the physical channels and physical masses of the particles. We shall make use of it too in order to investigate the isospin violation effects.

IV. AMPLITUDES IN OTHER STRANGENESS AND ISOSPIN CHANNELS.

For completeness we give here the $S = -1, T = 2$ and $S = 1$ channels, plus the $S = -1$ in K^-n and related channels.

a) $S = -1, T = 2$ channel:

Only the $\pi\Sigma$ state couples to this channel. We take $| \pi^+\Sigma^+ \rangle \equiv | 2, 2 \rangle$ and the potential in this case is given by

$$V = \frac{1}{2f^2}\,(k^0 + k'^0) \tag{10}$$

b) $S = 1$ channel.

We take K^+n and the coupled state K^0p, which are admixtures of $T = 0, T = 1$. The potential in this case is given by

$$V_{ij} = -\frac{1}{4f^2} \; L_{ij}(k^0 + k'^0) \tag{11}$$

with the L_{ij} coefficients given in Table IV.

The K^+p state stands alone for the $T = 1, T_3 = 1$ channel. The potential is given by

$$V = \frac{1}{2f^2} \; (k^0 + k'^0) \tag{12}$$

The isospin amplitudes are written immediately and we have

$$V(S = 1, T = 0) = 0$$
$$V(S = 1, T = 1) = \frac{1}{2f^2}(k^0 + k'^0) \tag{13}$$

As we can see, at lowest order the $S = 1, T = 0$ amplitude vanishes. When working with the physical masses of the K^+, K^0, p and n, the coupling of the channels breaks slightly this symmetry but still leads to a very small amplitude as we shall see.

c)$S = -1, K^-n$ and related channels.

For the purpose of K^- nucleus interaction we shall also need the K^-n amplitude which we evaluate here. The coupled channels in this case, which is only $T = 1$, are $K^-n, \pi^0\Sigma^-, \pi^-\Sigma^0, \pi^-\Lambda, \eta\Sigma^-$. Since the matrix elements of the potential satisfy isospin symmetry, these matrix elements are easily induced from section 3 and Tables II and III. We have

$$V_{ij} = -\tilde{C}_{ij} \frac{1}{4f^2} \; (k^0 + k'^0) \tag{14}$$

where the $\tilde{C}_{ij}$ coefficients are given in Table V.

V. COUPLED CHANNELS LIPPMANN SCHWINGER EQUATIONS

Following [12] we write the set of Lippmann Schwinger equations in the $\bar{K}N$ centre of mass frame

$$t_{ij} = V_{ij} + V_{il} \, G_l \, T_{lj} \tag{15}$$

where the indices i, j run over all possible channels and

$$V_{il} \, G_l \, T_{lj} = i \int \frac{d^4 q}{(2\pi)^4} \frac{M_l}{E_l(\vec{q})} \frac{V_{il}(k,q) \, T_{lj}(q,k')}{k^0 + p^0 - q^0 - E_l(\vec{q}) + i\epsilon} \frac{1}{q^2 - m_l^2 + i\epsilon} \tag{16}$$

Eq. (15) sums up automatically the series of diagrams of fig. 1. In eq. (16) we have kept the positive energy part of the baryon propagator, although with proper relativistic factors in order to ensure exact phase space in the imaginary part of the expressions. In eq. (16) M_l, E_l correspond to the mass and energy of the intermediate baryon and m_l to the mass of the intermediate meson.

The integral of eq. (16) is regularized through the use of a momentum cut off, q_{max}. The value of q_{max} is a free parameter of the theory by means of which one accounts for higher order contributions in an effective way.

Some other comments must be made with respect to the off shell extrapolation of $V_{il}(k,q)$ which run in parallel to the findings of [12]. In that work the potential was split into an on shell part plus a rest. The contribution from this latter part was found to go into renormalization of couplings and masses and could hence be omitted in the calculation. This simplified the coupled integral equations which became then ordinary algebraic equations. The same happens here, as we see below.

Let us take the one loop diagram of fig. 1 and equal masses in the external and intermediate states for simplicity. We have

$$\begin{aligned} V_{off}^2 &= C(k^0 + q^0)^2 = C(2k^0 + q^0 - k^0)^2 \\ &= C^2(2k^0)^2 + 2C(2k^0)(q^0 - k^0) + C^2(q^0 - k^0)^2 \end{aligned} \tag{17}$$

with C a constant. The first term in the last expression is the on shell contribution $V_{on}^2 (V_{on} \equiv C2k^0)$. Neglecting $p^0 - E(q)$ in eq. (16), typical approximations in the heavy baryon formalism [16], the one loop integral for the second term of eq. (17) becomes ($\omega(q)^2 = \vec{q}^2 + m^2$)

$$2iV_{on} \int \frac{d^3q}{(2\pi)^3} \int \frac{dq^0}{2\pi} \frac{M}{E(q)} \frac{q^0 - k^0}{k^0 - q^0} \frac{1}{q^{02} - \omega(q)^2 + i\epsilon} =$$
$$-2V_{on} \int \frac{d^3q}{(2\pi)^3} \frac{M}{E(q)} \frac{1}{2\omega(q)} \sim V_{on} \, q_{max}^2 \qquad (18)$$

As we can see this term is proportional to V_{on} and hence can be reabsorbed by a suitable renormalization of the coupling f. Therefore, the use of the physical coupling will incorporate this term. In the case of coupled channels the arguments are similar. The contribution of eq. (18) has the same structure as the lowest order terms and can be reabsorbed in the lowest order Lagrangian by a suitable renormalization, leading to the effective chiral Lagrangian with the physical couplings.

Similarly, the term proportional to $(q^0 - k^0)^2$ will cancell the $(k^0 - q^0)$ term in the denominator and the integral of this term, proportional to $(k^0 - q^0)$, gives rise to another term proportional to k^0 (and hence V_{on}) while the term proportional to q^0 vanishes for parity reasons.

We can extend these arguments to higher order loops and the conclusion is that we can factorize V_{on} and T_{on} outside the integral of eq. (16). Hence in matrix form we will have

$$T = V + V \, G \, T \qquad (19)$$

or equivalently

$$T = [1 - V \, G]^{-1} \, V \qquad (20)$$

with G a diagonal matrix given by

$$G_l = i \int \frac{d^4q}{(2\pi)^4} \frac{M_l}{E_l(\vec{q})} \frac{1}{k^0 + p^0 - q^0 - E_l(\vec{q}) + i\epsilon} \frac{1}{q^2 - m_l^2 + i\epsilon}$$
$$= \int \frac{d^3q}{(2\pi)^3} \frac{1}{2\omega_l(q)} \frac{M_l}{E_l(\vec{q})} \frac{1}{p^0 + k^0 - \omega_l(\vec{q}) - E_l(\vec{q}) + i\epsilon} \qquad (21)$$

which depends on $p^0 + k^0 = \sqrt{s}$ and q_{max}.

The method of [13] provides an alternative reinterpretation of the on shell factorization which is clarifying. The method uses the optical theorem to start with, which is stated here as

9

$$Im\,T = T\,Im\,G\,T^*$$ (22)

from where one deduces

$$Im\,G = -Im\,T^{-1}$$ (23)

Hence

$$T = [Re\,T^{-1} - i\,Im\,G]^{-1} =$$
$$V[V\,Re\,T^{-1}\,V - i\,V\,Im\,G\,V]^{-1}\,V$$ (24)

where in the last step we have multiplied twice by VV^{-1} for convenience, with $V \equiv V_{on}$. Expanding formally $V\,Re\,T^{-1}\,V$ in powers of a suitable parameter, proportional to k^0 for instance, one obtains up to 2nd order

$$T = V\,[V - Re\,T_2 - i\,V\,Im\,G\,V]^{-1}\,V$$ (25)

with T_2 the second term in the expansion of $T(T = T_1 + T_2,\ T_1 \equiv V)$. The freedom of the cut off can be used to make $Re\,T_2 \simeq V\,Re\,G\,V$, in which case eq. (25) reduces to the LS equations implicit in eq. (19). The success of the LS method in [12] suggests that the expansion of $V\,Re\,T^{-1}\,V$, and the approximation to $Re\,T_2$ given above, are sensible approximations at least in the scalar sector for the meson-meson interaction. One hopes that this is also the case for the meson-baryon interaction in $L = 0$ that we study here.

The coupled-channel equations represented by eq. (19) are solved in the isospin basis for the $T = 0$, $T = 1$ cases, from where the amplitudes in the physical channels are then constructed. Alternatively we can work directly with the physical states using the matrix of Table I and the physical masses of each particle. The second method is more accurate and respects exactly the thresholds for the reaction and the phase space. We use both methods and this allows us to see the amount of isospin violation in the different channels.

The channels $\eta\Lambda, \eta\Sigma$ are above threshold for low energies of the K^-. The potential $V_{ij}(s)$ for these channels is taken through an analytical continuation using the formula

$$k^0 = \frac{s + m_\eta^2 - M_B^2}{2\sqrt{s}}$$ (26)

10

VI. THE Λ (1405) RESONANCE AND THE $\pi\Sigma$ MASS SPECTRUM.

The $\Lambda(1405)$ resonance appears below the K^-p threshold. It is observed in the mass spectrum of $\pi\Sigma$. One of the reactions used to see it is $\pi^-p \to K^0\Sigma^+\pi^-$ [17].

According to [18], the mass distribution of the $\Sigma^+\pi^-$ state, for s-wave resonance, is given by

$$\frac{d\sigma}{dm_\alpha} = C|t_{\pi\Sigma\to\pi\Sigma}|^2 p_{CM} \tag{27}$$

where C is a constant, $t_{\pi\Sigma\to\pi\Sigma}$ is the $T = 0$ $\pi\Sigma$ amplitude and p_{CM} is the π momentum in the frame where $\pi\Sigma$ is at rest.

VII. RESULTS

With the normalization which we use, the cross section is given by

$$\sigma_{ij} = \frac{1}{4\pi}\frac{MM'}{s}\frac{k'}{k}|T_{ij}|^2 \tag{28}$$

The relationship to the scattering lengths in elastic channels reported in [8] is

$$a_i = -\frac{1}{4\pi}\frac{M}{\sqrt{s}}T_{ii} \tag{29}$$

calculated at threshold.

We look at the cross sections for $K^-p \to K^-p, \bar{K}^0n, \pi^0\Lambda, \pi^0\Sigma^0, \pi^+\Sigma^-, \pi^-\Sigma^+$ at low energies plus the $\pi\Sigma$ mass distribution and the threshold branching ratios. Our free parameter is q_{max}, but we allow also some small variation of f from the pionic value of $f_\pi = 93$ MeV. For kaons in the meson-meson interaction $f_K = 1.22f_\pi$ and we should expect a similar renormalization here. However, for simplicity, we use a single value of f for pions and kaons which is fit to the data and turns out to be between f_π and f_K.

The threshold branching ratios which we use in the fitting procedure, as in [8], are [19,20]:

$$\gamma = \frac{\Gamma(K^-p \to \pi^+\Sigma^-)}{\Gamma(K^-p \to \pi^-\Sigma^+)} = 2.36 \pm 0.04$$

$$R_c = \frac{\Gamma(K^-p \to \text{charged particles})}{\Gamma(K^-p \to \text{all})} = 0.664 \pm 0.011 \tag{30}$$

$$R_n = \frac{\Gamma(K^-p \to \pi^0\Lambda)}{\Gamma(K^-p \to \text{all neutral states})} = 0.189 \pm 0.015$$

Note that the ratio γ is zero in lowest order of the chiral Lagrangians (see Table I). The coupled-channel LS equations lead to a finite cross section for $K^-p \to \pi^+\Sigma^-$ which is larger than the $K^-p \to \pi^-\Sigma^+$ as we shall see.

Our fitting procedure proceeds as follows: first we fix a value of f around $f_\pi = 93$ MeV and vary q_{max} in order to get the best reproduction of the threshold parameters, γ, R_c, R_n. There is a correlation between the values of q_{max} and f leading to the best fit to these threshold parameters. A 2% increase in f can be compensated with a 3% increase in q_{max}. The shape and position of the $\Lambda(1405)$ resonance depend on the value of f (and its associated q_{max} from the previous fit) and we choose the value of f which leads to the best agreement with the $\Lambda(1405)$ properties seen in the $\pi\Sigma$ mass spectrum. This procedure determines f, q_{max} and no further input is used in the fit. The cross sections are then calculated with the best choice of parameters and have not not been used in a best fit to the data. As we shall see, it is a remarkable feature of this chiral coupled-channel approach that the threshold ratios plus the position and shape of the $\Lambda(1405)$ determine the behaviour of the K^-p cross sections at low energies in all channels.

Our optimal choice was found for $f = 1.15f_\pi, q_{max} = 630$ MeV. The following results are evaluated inverting the 8×8 matrix $(1 - V G)$ with V given in Table I. We will also show the results obtained using the isospin basis and inverting $(1 - V G)$ with V given by Tables II and III. At the same time we show the results obtained omitting the $\eta\Lambda$ and $\eta\Sigma^0$ channels as done in [8].

In fig. 2 we show the $\pi\Sigma$ spectrum corresponding to the $\Lambda(1405)$ resonance. As we can see, the peak position and width are well reproduced. The results obtained using the isospin basis and those omitting the η channels are also shown in the figure. The results with

the isospin basis are similar to those obtained with the basis of physical states, however, omitting the η channels leads to a quite different mass distribution, which is incompatible with the data. Obviously one can choose other values of f and q_{max} to reproduce the mass distribution without the η channels but, as shown in [8] and corroborated here, one can not obtain a global fit to the data. In any case, one of the points in this paper is to show the relevance of the inclusion of the η channels in the coupled-channel equations, and the results for the $\Lambda(1405)$ resonance are a clear example of it, although more spectacular effects on other observables will be shown in the following.

In Table VI we display the results for the threshold ratios evaluated in the three cases: isospin basis, full basis and omitting η channels. We can see that the three ratios are reproduced within 5% in the calculation with the full basis. Note that using the isospin basis or omitting the η channels produces appreciable changes in these ratios. Particularly remarkable is the change in the ratio γ, which is reduced by a factor 2.2 when the η channels are omitted. It is worth mentioning that the small values for γ obtained in [8], which are compatible with our value when the η channels are omitted, motivated the authors of that work to introduce higher order terms in the chiral expansion and perform a global fit with five parameters.

In figs. 3–8 we compare our cross sections with the low-energy scattering data [21–26]. We show the results obtained with the full basis of eight physical coupled states (full line), with the isospin basis (short-dashed line) and omitting the η channels (long-dashed line). The elastic cross section $K^-p \to K^-p$ is displayed in fig. 3. The cross section calculated with the isospin basis is about 25% higher at low energies than the one evaluated using the basis of physical states. Another interesting feature is the cusp appearing around the K^- lab momentum $p_L = 90$ MeV/c in the full basis calculation, which corresponds to the opening of the $\bar{K}^0 n$ channel. This cusp appears weakened and at lower energies in the calculation with the isospin basis as a consequence of the use of average masses for $\bar{K}$, π, N and Σ. More spectacular is the effect of omitting the $\eta\Lambda, \eta\Sigma$ channels which leads to a 60% larger K^-p elastic cross section close to threshold and about 40% larger around $p_L = 100$ MeV/c.

In fig. 4 we show the cross section for $K^- p \to \bar{K}^0 n$. The results for the isospin basis calculation and those using the full basis are nearly identical. Omitting the $\eta \Lambda$ and $\eta \Sigma$ channels in this case reduces the cross section in 20% around $p_L = 130$ MeV/c and above.

In fig. 5 we show the cross section for $K^- p \to \pi^0 \Lambda$. In this case the use of the isospin basis nearly doubles the cross section close to threshold with respect to the results with the full basis. The effects of omitting the $\eta \Lambda, \eta \Sigma$ channels are more moderate here and amount to an increase of about 20% in the region of the cusp and about 10% at momenta higher than $p_L = 140$ MeV/c.

In fig. 6 we show the cross section for $K^- p \to \pi^+ \Sigma^-$. The results using the isospin basis are about 45% larger close to threshold than those obtained with the full basis. The effects of omitting the η channels are moderate and result into an increase of the cross section of about 12% close to threshold and a negligible change for $p_L > 100$ MeV/c.

In fig. 7 we show the cross section for $K^- p \to \pi^0 \Sigma^0$. Although not visible in the figure, the cross section at energies close to threshold using the isospin basis is about 25% higher than the one obtained with the full basis. Omitting the η channels increases the cross section in about 60% close to threshold and in about 30% at $p_L \simeq 100$ MeV/c.

Finally, in fig. 8 we show the results for the $K^- p \to \pi^- \Sigma^+$ reaction. The cross sections at threshold with the isospin and the full bases are similar, but the latter results show a very pronounced cusp around $p_L = 90$ MeV/c corresponding to the opening of the $\bar{K}^0 n$ channel. This cusp is shifted to lower energies and is less aparent in the case of the isospin basis. The omission of the η channels has in this case a spectacular effect. The cross section is multiplied by a factor of nearly three close to threshold when the η channels are omitted. As a consequence the threshold ratio γ is very sensitive to the η channels as is evident from the results in Table VI. Around $p_L = 100 - 150$ MeV/c the cross section omitting the η channels is about twice as large as the full calculation.

One of the novel findings of the present work is that the inclusion of the η channels is very important and allows one to obtain a good reproduction of the data by means of the lowest order Lagrangian alone using a cut off, q_{max}, and changing f moderately from the f_π

14

value of the meson-meson interaction.

In fig. 9, following the parallelism with the work of [8], we show the amplitudes for $K^-p \rightarrow K^-p$ and $K^-n \rightarrow K^-n$ calculated with the full basis of physical states and including the η channels. The results are similar to those obtained in [8].

In Table VII we show the scattering lengths for K^-p and K^-n calculated with the three methods. We observe that isospin breaking effects in the K^-n amplitude, as well as those omitting the η channel, are moderate in this case. We shoud note that this is a $T = 1$ channel where the $\Lambda(1405)$ resonance is not present. However, the K^-p amplitude, which is affected by the presence of the resonance, shows a larger sensitivity to isospin breaking effects and the η channels.

The K^-p scattering length is also in good agreement with the one obtained in [8]. However, the results obtained with the isospin basis are closer to those obtained in the full basis in our case, while in [8] $Re(a)$ is about a factor two smaller when average masses for K and N are used.

Our results for the K^-p scattering length are essentially in agreement with the most recent results from Kaonic hydrogen X rays [27], $(-0.78\pm0.15\pm0.03)+i(0.49\pm0.25\pm0.12)$ fm, and in qualitative agreement with the scattering length determined from scattering data in [28], $(-0.67+i\,0.64)$ fm with 15% estimated error. These latter results are obtained from the isospin scattering lengths determined in [28], but as we can see from Table VII there are violations of isospin at the level of 20% in these amplitudes.

The K^-n scattering length is also in qualitative agreement with the $T = 1$ value of [28], $(0.37 + i\,0.60)$ fm with also 15% estimated errors.

It is also worth calling the attention to the remarkable agreement of our results for the real part of the scattering lengths with those obtained in [28] from a combined dispersion relation and M matrix analysis, $Re(a_{K^-p}) = -0.98$ fm, $Re(a_{K^-n}) = 0.54$ fm.

Next we look at the $S = 1$ sector. In fig. 10 we show the phase shifts in the isospin channel $T = 1$. The agreement with experiment [29] is fair but the phase shifts in absolute value are a little smaller than experiment. This result is qualitatively similar to the one

obtained in [8], where it was also shown that allowing for a K^+p shorter range parameter (larger cut off in our case) the agreement with data improves.

On the other hand the scattering length in $T = 0$, which was zero at lowest order (eq. (13)), becomes finite, although negligibly small, as a consequence of the coupling to other channels when the different masses are kept. We obtain a value

$$a(S = 1, T = 0) = 2.4 \times 10^{-7} \text{ fm} \tag{31}$$

which is compatible with present experimental data, 0.02 ± 0.04 fm [30]. We also evaluate the scattering length for K^+N in $T = 1$, for which we get

$$a(S = 1, T = 1) = -0.26 \text{ fm} \tag{32}$$

which compares reasonably with the experimental number -0.32 ± 0.02 fm [30]. The discrepancy is similar to the one obtained for the phase shifts in fig. 10. For completeness we also show the phase shifts for $S = -1, T = 2$ in fig. 11.

VIII. DISCUSSION AND CONCLUSIONS

We have presented here a method of coupled-channel Lippmann Schwinger equations which allows us to evaluate the $L = 0$ amplitudes and obtain a good description of the $K^-p \to K^-p, \bar{K}^0n, \pi^0\Lambda, \pi^0\Sigma^0, \pi^+\Sigma^-, \pi^-\Sigma^+$ cross sections at low energies plus the properties of the $\Lambda(1405)$ resonance. The method uses as input only the lowest order chiral Lagrangian which is used as a source of the potential in the LS equations, and a cut off to regularize the loop integrals.

Using different argumentations we showed that in the loop evaluation only the on-shell part of the potential was needed, which reduced the coupled-channel integral equations to algebraic equations. The approach is more economical than the one of [8] in which it was inspired. Here one obtains a good reproduction of the data without the need to use the information from higher order Lagrangians. We should note that the parameters of these

Lagrangians do not have a fixed value. They depend upon the energy scale chosen for the regularization [1]. In our language this means that they depend upon the cut off q_{max} which plays a similar role to the energy scale in the dimensional regularization of [1]. The success of our method using only the lowest order Lagrangian implies that the chosen cut off minimizes the effect of the higher order Lagrangians in the L = 0 channel that we have studied. The same thing happened in the meson-meson interaction in $L = 0$ [12]. In [8] a form factor is used with a range similar to our cut off, but a solution using only the lowest order Lagrangians could not be found. Although a fair reproduction of the cross sections and $\pi\Sigma$ mass distribution could be found, the threshold parameters, particularly γ, were very poorly reproduced. We have reconfirmed these findings omitting the $\eta\Lambda, \eta\Sigma$ channels in the coupled-channel system. However, and this is one of the main findings of the present work, the situation is drastically changed when these channels are included. The ratio γ is increased by about a factor 2.2, coming in good agreement with the data, and an appreciable change in all the channels is induced, particularly in the $K^-p \to K^-p, \pi^0\Sigma^0$ reactions, and most specially in the $K^-p \to \pi^-\Sigma^+$ reaction whose cross section is reduced in about a factor three at small energies.

As commented above, our fit to the data was done only for the threshold ratios and the $\Lambda(1405)$ properties. This determined f and q_{max}. The value $f = 1.15f_\pi$ obtained in the best fit lies between f_π and f_K in the meson-meson interaction and appears as a reasonable renormalization of f_π in the $\bar{K}N$ sector. The cross sections were not used for the fit. In spite of that, it is remarkable to see the agreement of the results obtained with the data. The cross sections for the $K^-p \to K^-p, \bar{K}^0n, \pi^+\Sigma^-, \pi^0\Sigma^0$ are in very good agreement with the data. Those for the $K^-p \to \pi^-\Sigma^+$ are also compatible with the data within errors, with small discrepancies in the deep region around $k = 90$ MeV/c largely influenced by a cusp effect in our case. Only the $K^-p \to \pi^0\Lambda$ cross section appears to overestimate slightly the scarce available data.

The success of our approach in $\bar{K}N$ and coupled channels for $L = 0$ with the lowest order Lagrangian and a cut off does not mean that the procedure can be generalized to

all meson-nucleon channels. The richness of this information most probably requires the use of higher order Chiral Lagrangians, as it was the case in the meson-meson interaction when including all different channels [13]. For the purpose of determining these higher order terms, for a chosen scale of energies in the regularization scheme (cut off in our method), a global fit to all meson-nucleon data would have to be conducted in analogy to the work of [13].

Meanwhile, the success of our scheme, wich is quite economical, could be exploited to address problems related with the propagation of kaons in matter, a topic which has aroused much interest lately [7,31–33].

ACKNOWLEDGMENTS

REFERENCES

[1] J. Gasser and H. Leutwyler, Nucl. Phys. B250 (1985) 465

[2] U. G. Meissner, Rep. Prog. Phys. 56 (1993) 903

[3] A. Pich, Rep. Prog. Phys. 58 (1995) 563

[4] G. Ecker, Prog. Part. Nucl. Phys. 35 (1995) 1

[5] V. Bernard, N. Kaiser and U. G. Meissner, Int. J. Mod. Phys. E4 (1995) 193

[6] C. H. Lee, H. Jung, D. P. Min and M. Rho, Phys. Lett. B326 (1994) 14

[7] G. E. Brown, C. H. Lee, M. Rho and V. Thorsson, Nucl. Phys. A567 (1994) 937

[8] N. Kaiser, P. B. Siegel and W. Weise, Nucl. Phys. A594 (1995) 325

[9] N. Kaiser, T. Waas and W. Weise, Nucl. Phys. A612 (1997) 297

[10] C. H. Lee, D. P. Min and M. Rho, Nucl. Phys. A602 (1996) 334

[11] P.B. Siegel and B. Saghai, Phys. Rev. C52 (1995) 392

[12] J. A. Oller and E. Oset, Nucl. Phys. A620 (1997) 438

[13] J. A. Oller, E. Oset and J. R. Peláez, Univ. Valencia preprint 1997

[14] A. Dobado, M. J. Herrero and T. N. Truong, Phys. Lett. B235 (1990) 129

[15] A. Dobado and J. R. Peláez, Phys. Rev. D47 (1992) 4883; ibid. D56 (1997) 3057

[16] E. Jenkins and A. V. Manohar, Phys. Lett. B255 (1991) 558

[17] D. W. Thomas, A. Engler, H. E. Fisk and R. W. Kraemer, Nucl. Phys. B56 (1973) 15;
    R. J. Hemingway, Nucl. Phys. B253 (1985) 742

[18] S. M. Flatté, Phys. Lett. B63 (1976) 224

[19] R. J. Nowak et al., Nucl. Phys. B139 (1978) 61

[20] D. N. Tovee et al., Nucl. Phys. B33 (1971) 493

[21] W.E. Humphrey and R.R. Ross, Phys. Rev. 127 (1962) 1305

[22] M. Sakitt et al., Phys. Rev. 139 (1965) 719

[23] J. K. Kim, Phys. Rev. Lett. 21 (1965) 29; J. K. Kim, Columbia University Report, Nevis 149 (1966)

[24] W. Kittel, G. Otter and I. Wacek, Phys. Lett. 21 (1966) 349

[25] J. Ciborowski et al., J. Phys. G8 (1982) 13

[26] D. Evans et al., J. Phys. G9 (1983) 885

[27] M. Iwasaki et al., Phys. Rev. Lett. 78 (1997) 3067

[28] A. D. Martin, Nucl. Phys. B179 (1981) 33

[29] B. R. Martin, Nucl. Phys. B94 (1975) 413

[30] See C. Dover and G. Walker, Phys. Reports 89 (1982) 1 for a compilation of data.

[31] T. Waas, N. Kaiser and W. Weise, Phys. Lett. B365 (1996) 12

[32] G. E. Brown, K. Kubodera, M. Rho and V. Thorsson, Phys. Lett. B291 (1992) 355

[33] C. H. Lee, G. E. Brown, D. P. Min and M. Rho, Nucl. Phys. A385 (1995) 481

TABLES

TABLE I. C_{ij} coefficients of eq. (7). $C_{ji} = C_{ij}$.

	K^-p	$\bar{K}^0n$	$\pi^0\Lambda$	$\pi^0\Sigma^0$	$\eta\Lambda$	$\eta\Sigma^0$	$\pi^+\Sigma^-$	$\pi^-\Sigma^+$
K^-p	2	1	$\frac{\sqrt{3}}{2}$	$\frac{1}{2}$	$\frac{3}{2}$	$\frac{\sqrt{3}}{2}$	0	1
$\bar{K}^0n$		2	$-\frac{\sqrt{3}}{2}$	$\frac{1}{2}$	$\frac{3}{2}$	$-\frac{\sqrt{3}}{2}$	1	0
$\pi^0\Lambda$			0	0	0	0	0	0
$\pi^0\Sigma^0$				0	0	0	2	2
$\eta\Lambda$					0	0	0	0
$\eta\Sigma^0$						0	0	0
$\pi^+\Sigma^-$							2	0
$\pi^-\Sigma^+$								2

TABLE II. D_{ij} coefficients of eq. (9) for $T = 0$. $D_{ji} = D_{ij}$.

	$\bar{K}N$	$\pi\Sigma$	$\eta\Lambda$
$\bar{K}N$	3	$-\sqrt{\frac{3}{2}}$	$\frac{3}{\sqrt{2}}$
$\pi\Sigma$		4	0
$\eta\Lambda$			0

TABLE III. F_{ij} coefficients of eq. (9) for $T = 1$. $F_{ji} = F_{ij}$.

	$\bar{K}N$	$\pi\Sigma$	$\pi\Lambda$	$\eta\Sigma$
$\bar{K}N$	1	-1	$-\sqrt{\frac{3}{2}}$	$-\sqrt{\frac{3}{2}}$
$\pi\Sigma$		2	0	0
$\pi\Lambda$			0	0
$\eta\Sigma$				0

TABLE IV. L_{ij} coefficients for $S = -1$. $L_{ji} = L_{ij}$.

	K^+n	K^0p
K^+n	-1	-1
K^0p		-1

TABLE V. $\tilde{C}_{ij}$ coefficients for K^-n and related channels in the $S = -1, T = 1$ sector. $\tilde{C}_{ji} = \tilde{C}_{ij}$.

	K^-n	$\pi^0\Sigma^-$	$\pi^-\Sigma^0$	$\pi^-\Lambda$	$\eta\Sigma^-$
K^-n	1	$\frac{1}{\sqrt{2}}$	$-\frac{1}{\sqrt{2}}$	$\sqrt{\frac{3}{2}}$	$\sqrt{\frac{3}{2}}$
$\pi^0\Sigma^-$		0	-2	0	0
$\pi^-\Sigma^0$			0	0	0
$\pi^-\Lambda$				0	0
$\eta\Sigma^-$					0

TABLE VI. Threshold ratios

	γ	R_c	R_n
Isos. basis	3.37	0.626	0.297
Full basis	2.33	0.640	0.217
No η	1.05	0.649	0.164
exp. [19,20]	2.36 ± 0.04	0.664 ± 0.011	0.189 ± 0.015

TABLE VII. $K^- N$ scattering lengths

	$a_{K^- p}$[fm]	$a_{K^- n}$[fm]
Isos. basis	$-0.85 + i1.24$	$0.54 + i0.54$
Full basis	$-0.99 + i0.97$	$0.53 + i0.61$
No η	$-0.64 + i1.66$	$0.47 + i0.53$
[8]	$-0.97 + i1.1$	
exp. [27]	$(-0.78 \pm 0.18) + i(0.49 \pm 0.37)$	
exp. [28]	$-0.67 + i0.64$	$0.37 + i0.60$
exp. $Re\,(a)$ [28]	-0.98	0.54

FIGURES
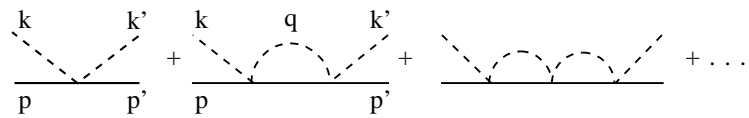
FIG. 1. Diagrammatic representation of the Lippmann Schwinger equations, eq. (15), in $\bar{K}N$ scattering.
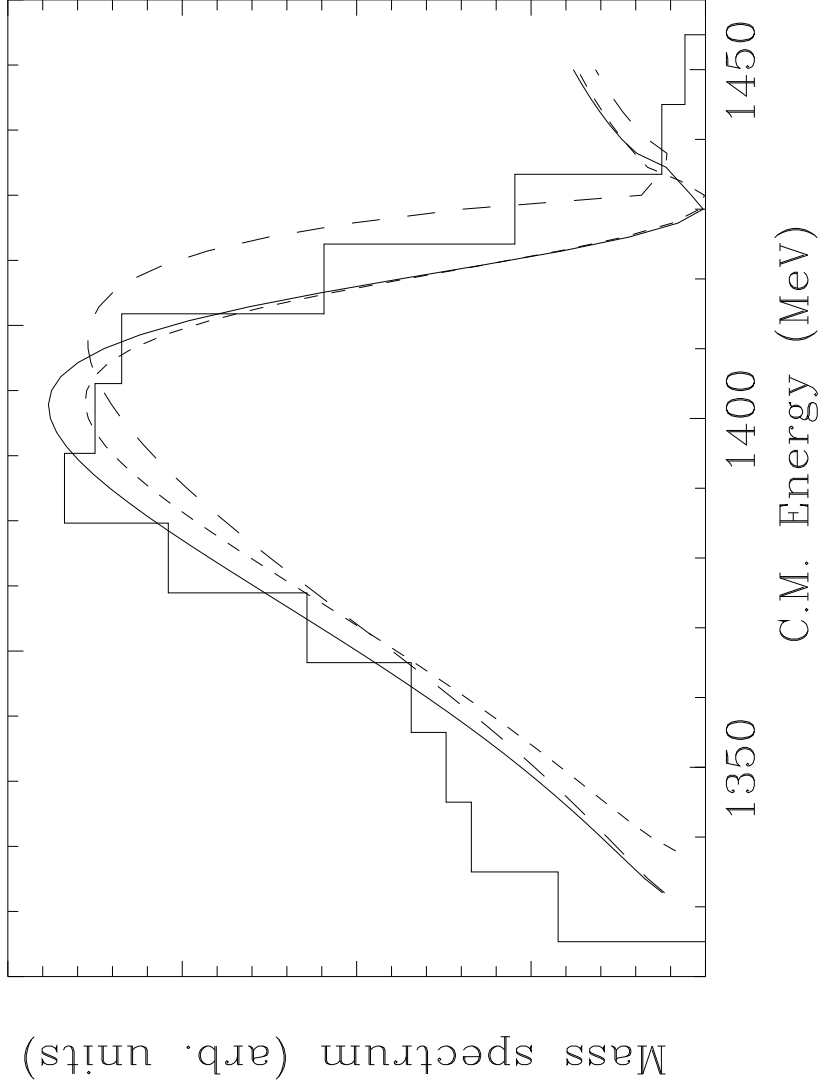
FIG. 2. The $\pi\Sigma$ mass distribution around the $\Lambda(1405)$ resonance from eq. (27). Short-dashed line: results in isospin basis. Long-dashed line: results omitting the $\eta\Sigma^0, \eta\Lambda$ channels. Full line: results with the full basis of physical states. Experimental data from [17].
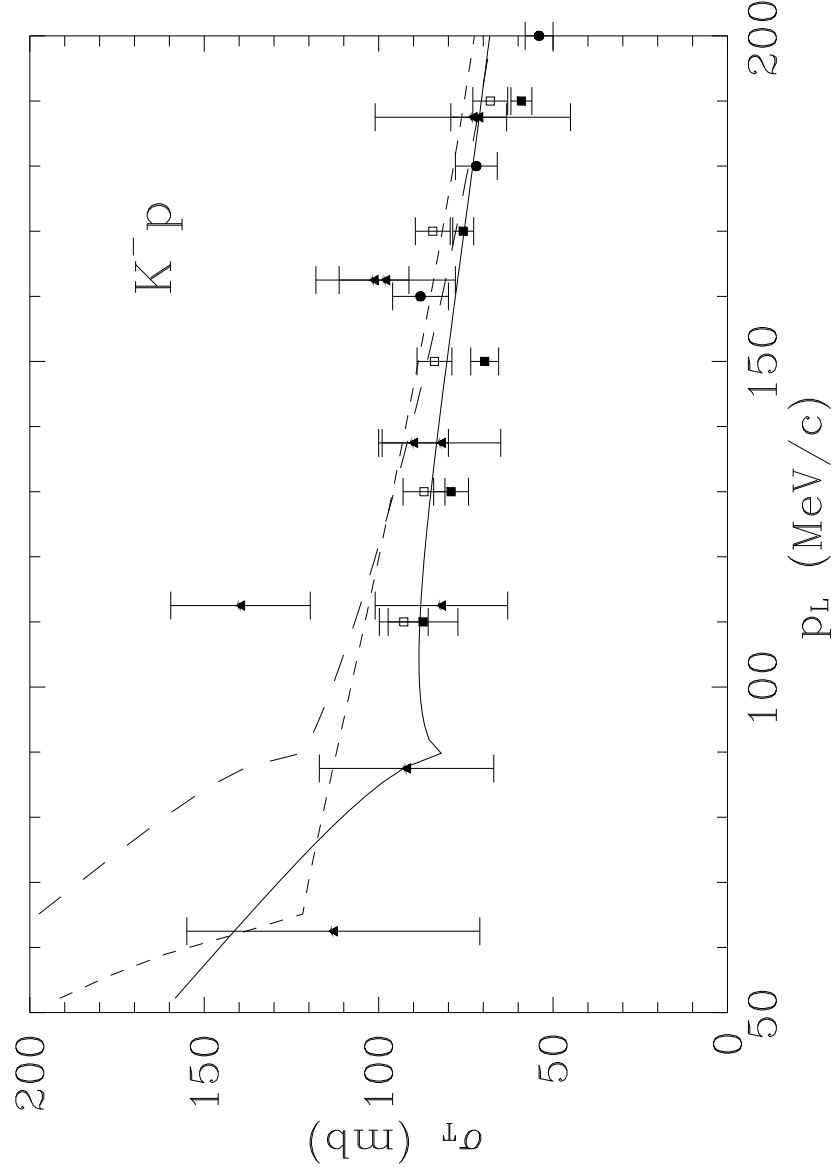
FIG. 3. $K^-p \rightarrow K^-p$ cross section as a function of the K^- momentum in the lab frame. Short-dashed line: results in isospin basis. Long-dashed line: results omitting the $\eta\Sigma^0, \eta\Lambda$ channels. Full line: results with the full basis of physical states. For Figs. 3–8, the experimental data are from: [21] (black triangles), [22] (black squares), [23] (open squares), [24] (open triangles), [25] (black circles) and [26] (open circles).
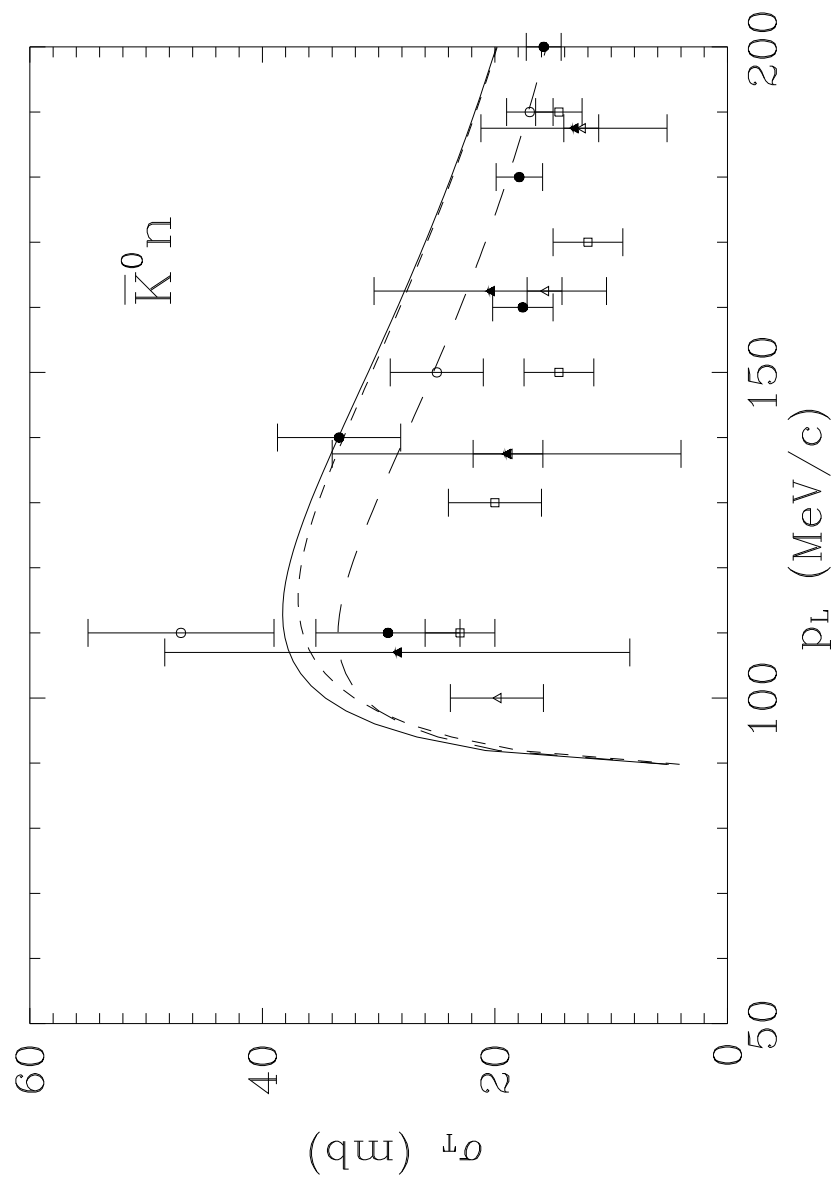
FIG. 4.   Same as fig. 3 for $K^-p \to \bar{K}^0 n$
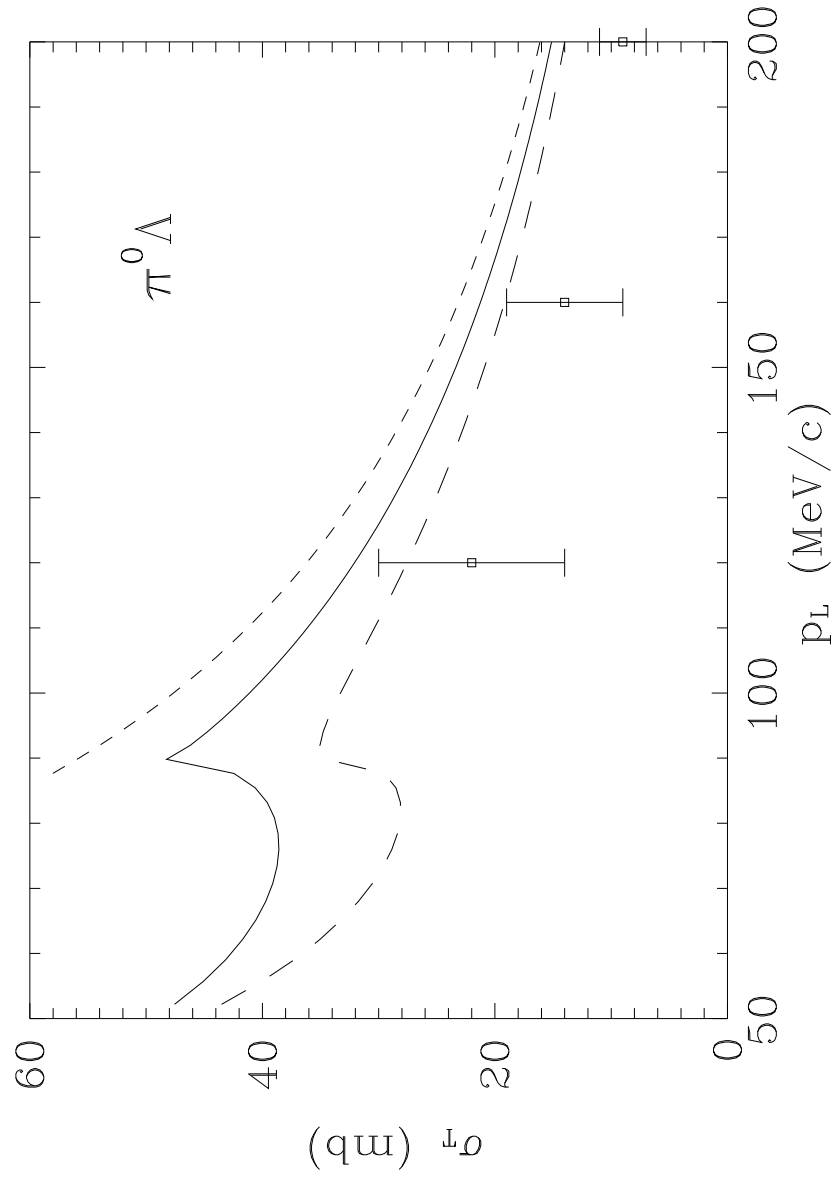
FIG. 5.   Same as fig. 3 for $K^-p \to \pi^0\Lambda$
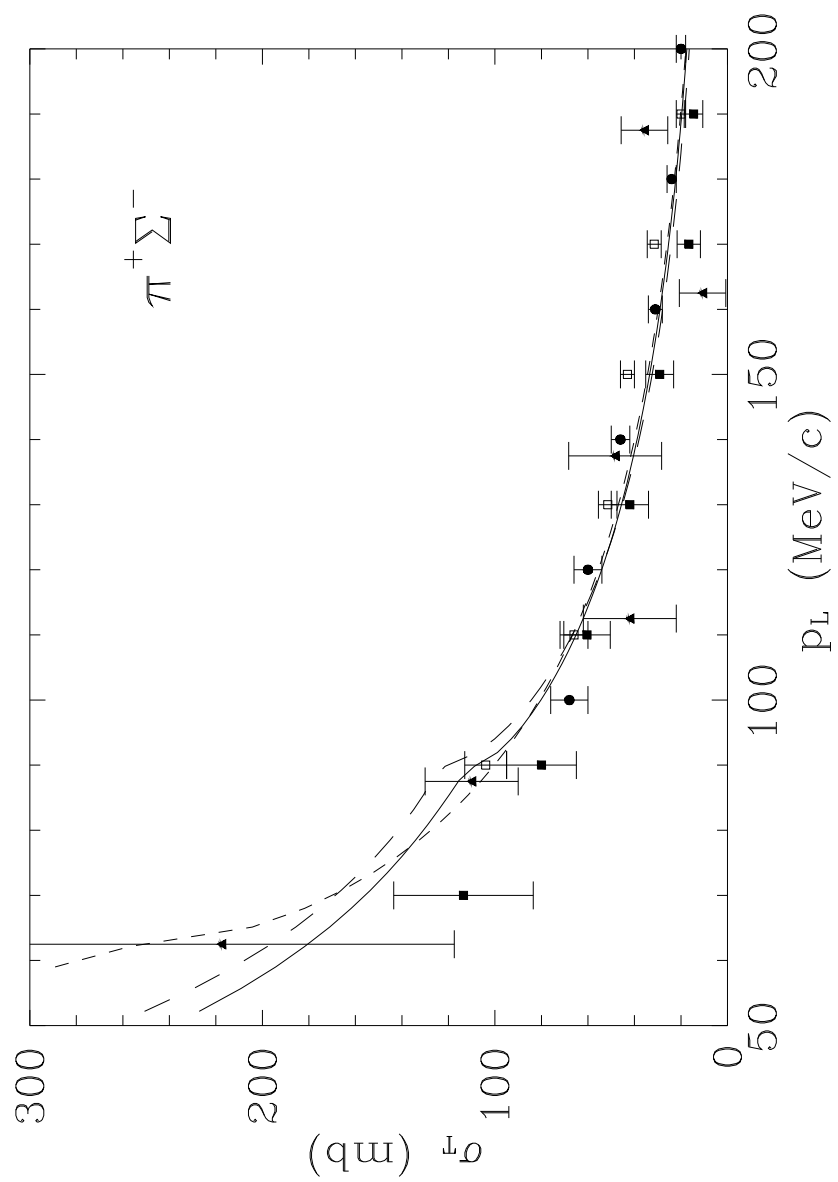
FIG. 6.   Same as fig. 3 for $K^-p \to \pi^+\Sigma^-$
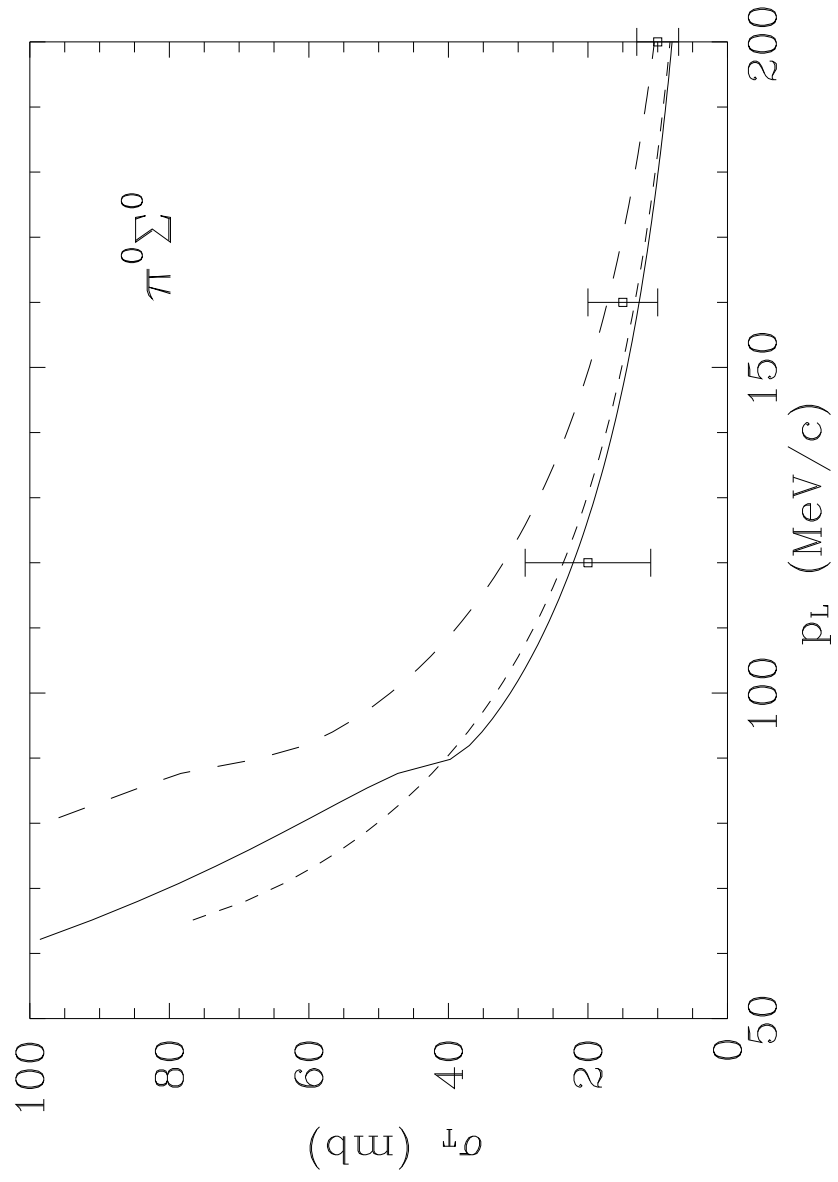
FIG. 7.   Same as fig. 3 for $K^- p \to \pi^0 \Sigma^0$
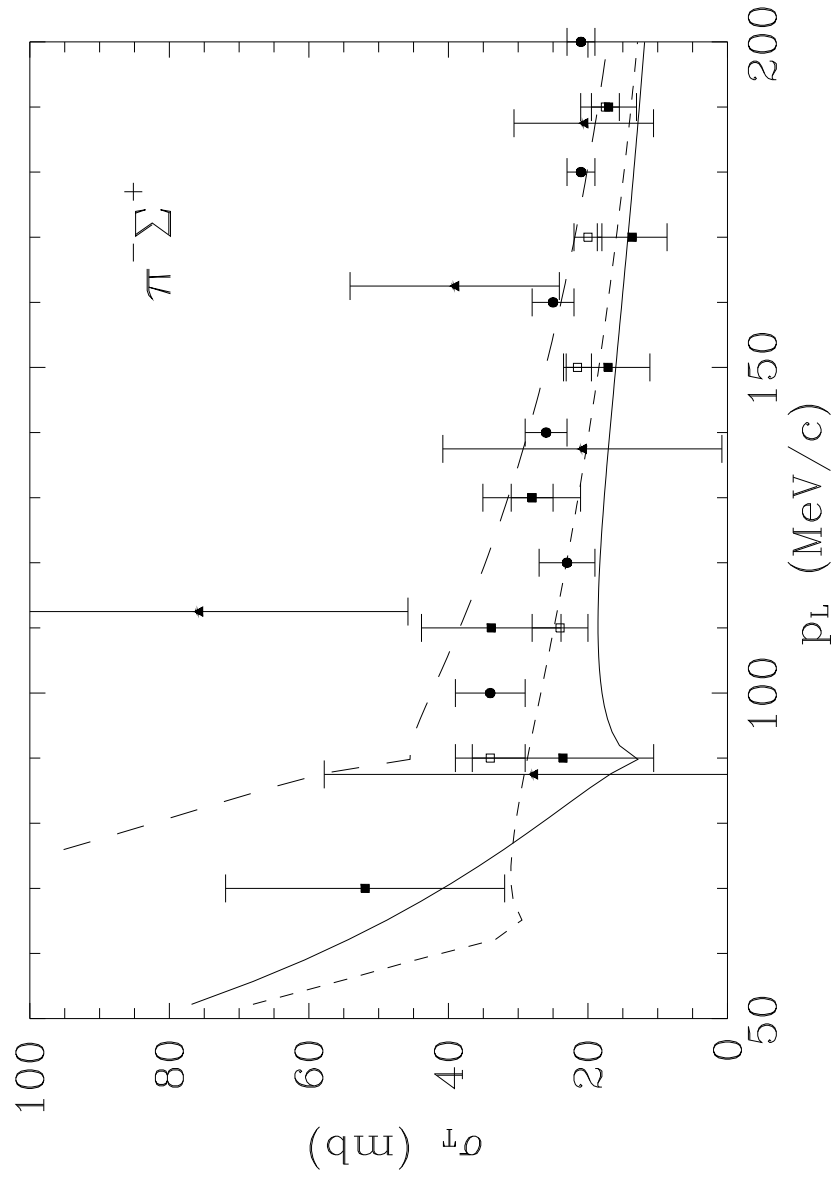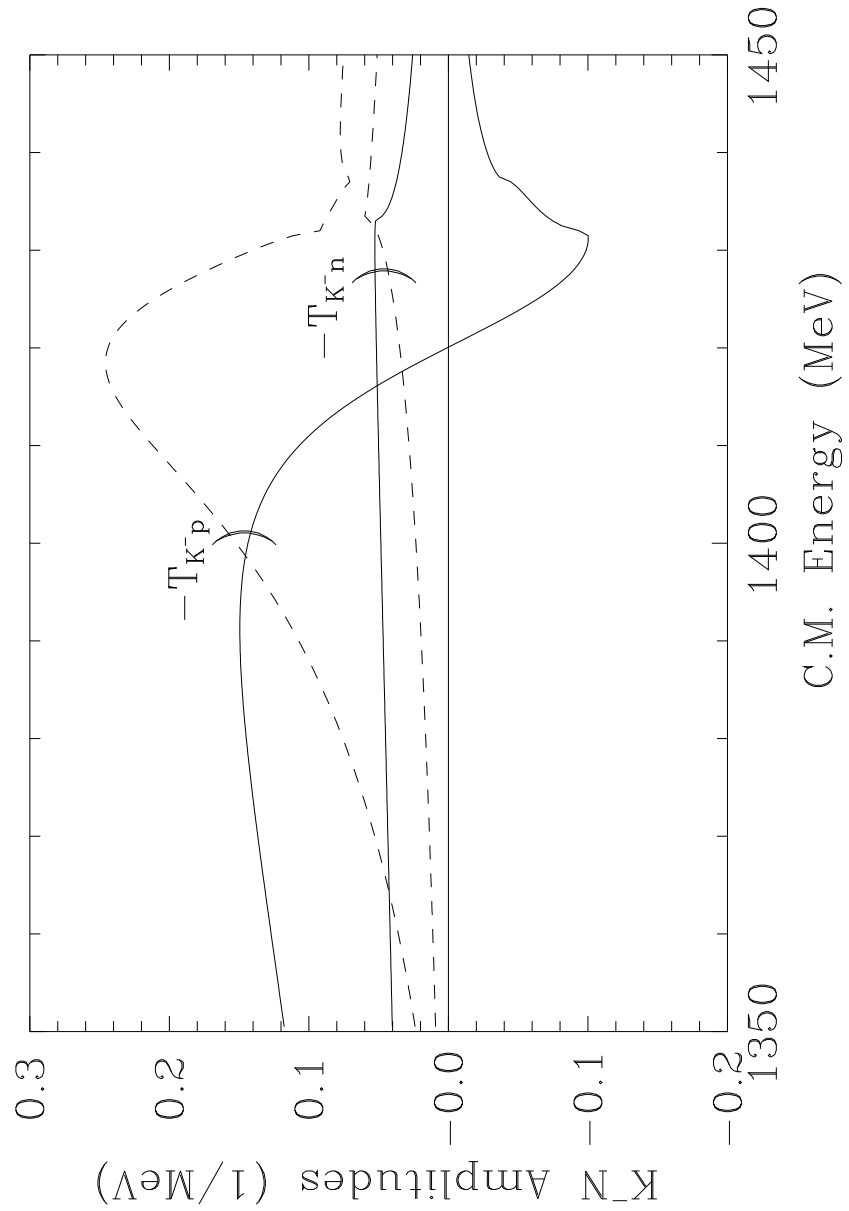
FIG. 8.   Same as fig. 3 for $K^-p \to \pi^-\Sigma^+$

FIG. 9. Scattering amplitudes for $K^-p \to K^-p$ and $K^-n \to K^-n$ around and below the K^-N threshold. Solid lines: real part. Dashed lines: imaginary part.
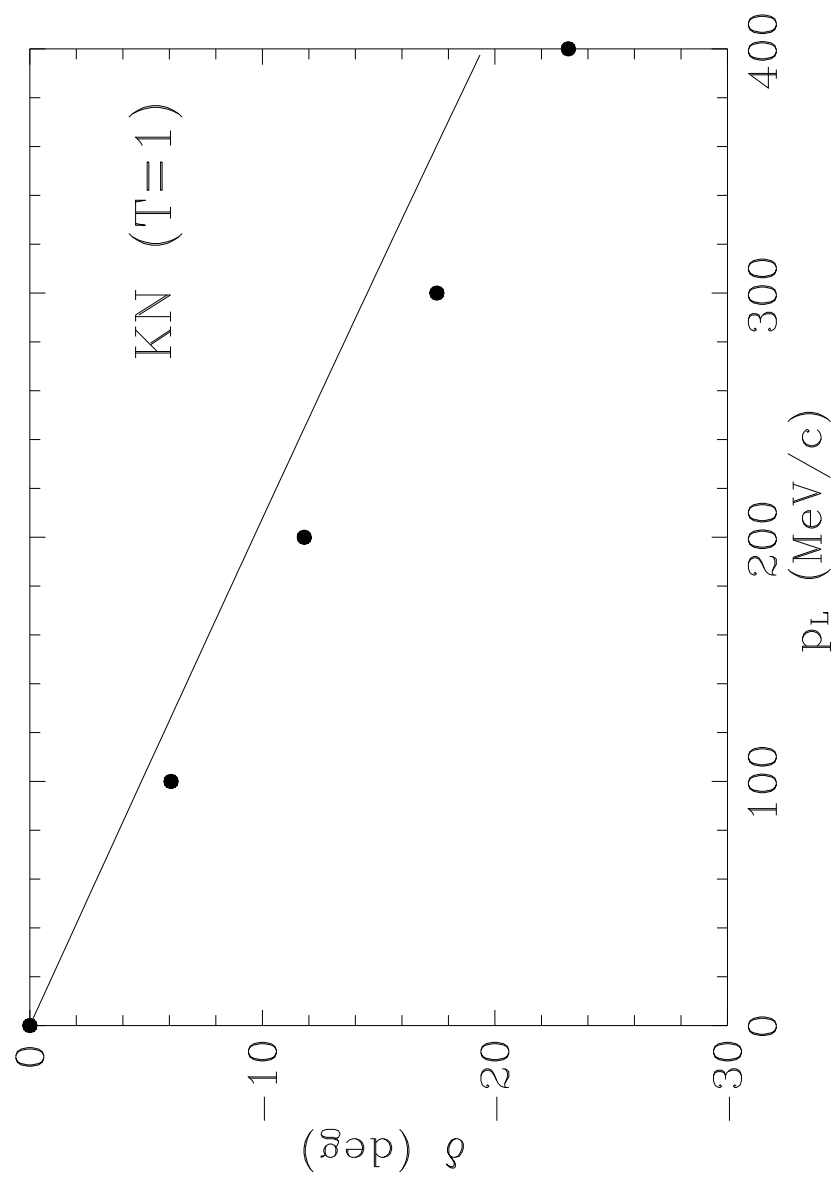
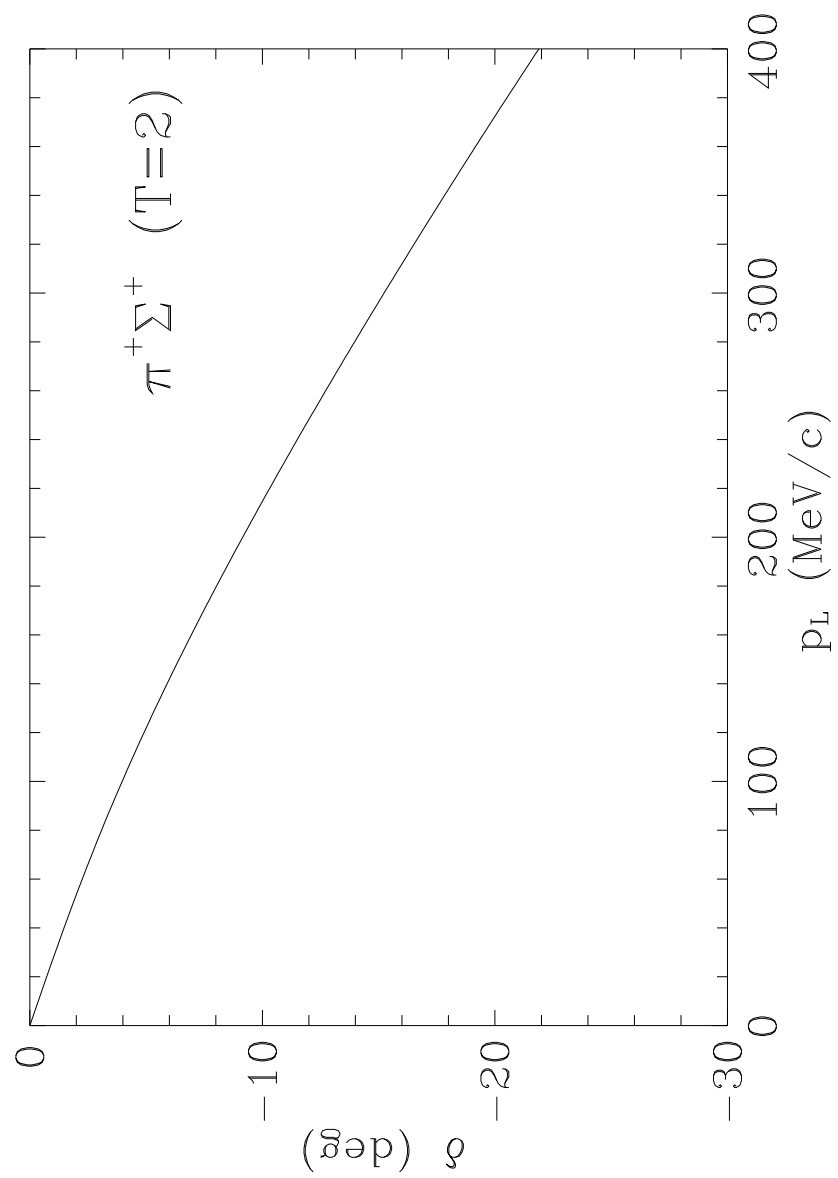FIG. 10.   S-wave phase shifts for KN in $T = 1$ as a function of the kaon lab momentum.

FIG. 11. S-wave phase shifts for $\pi^+\Sigma^+$ as a function of the pion lab momentum.